Tectonophysics, 65 (1980) 151—180

DEFORMATION PATTERN IN A HETEROGENEOUS MATERIAL: FOLDED AND CLEAVED SEDIMENTARY COVER IMMEDIATELY OVERLYING A CRYSTALLINE BASEMENT (OISANS, FRENCH ALPS)

JEAN-PIERRE GRATIER and PIERRE VIALON

Institut de Recherches Interdisciplinaires de Géologie et de Mécanique, Université I de Grenoble, B.P. 53X-F-38041, Grenoble Cedex (France)

(Received November 23, 1978; revised version accepted April 9, 1979)

ABSTRACT

Gratier, J.P. and Vialon, P., 1980. Deformation pattern in a heterogeneous material: folded and cleaved sedimentary cover immediately overlying a crystalline basement (Oisans, French Alps). Tectonophysics, 65: 151—179.

Particularly well exposed structures in folded and cleaved sedimentary cover immediately overlying a crystalline basement have been studied. Chemical analysis (X.R.F. and microprobe) reveal pressure solution process and give the possibilities of measurement of mass transfer. Study of fluid inclusion veins has determined the temperature pressure conditions: thermal effect of the basement and decrease of temperature and pressure with the age of various synkinematic veins.

Characteristic examples of the behaviour of a heterogeneous material during coaxial and non-coaxial deformation are shown:

(1) Successive different asymmetrical folds, various cleavages and fractures appear in a shear zone parallel to the main fabric with variations of thickness and rock behaviour.

(2) Evolution of cleavage in such a shear zone (with or without slipping) is linked to the relations between the rotation of contraction direction and the rate of the cleavage process.

(3) Fold axes changed from the horizontal Y direction to the vertical (or E—W transversal to the crystalline massif) X direction, with increase of the (X/Z) and (X/Y) ratios (obtained by fossils and reconstructed fold shape). This strain is always heterogeneous and the most deformed zone frequently evolves to discontinuities with slip.

(4) Indentation exists on all scale: from hard object (100 μ, with parenthesis form of pressure solution cleavage apparent on map distribution of various element) to basement block (with variation of strain value in the indented cover).

A model of the evolution of the deformation of sedimentary cover immediately overlying a crystalline basement is given in conclusion.

INTRODUCTION

The folded and cleaved Jurassic and Cretaceous formations, forming the cover of the external crystalline massif of Oisans (French Alps), exhibit par-

ticularly well-exposed structures due to deformation of heterogeneous multilayered rocks.

The aim of this paper is to present some characteristic examples of the behaviour of this material during coaxial and non-coaxial deformation. Various markers of deformation have been studied and measured and sometimes used to obtain local finite strain (fold shapes, deformed fossils). Comparative chemical analyses reveal pressure solution processes. Studies of fluid inclusions of various synkinematic veins have determined the temperature—pressure conditions of the deformation, these being particularly heterogeneous due to the thermal effect of the basement.

Because of inhomogeneity of deformation, the obtained strain values are only comparative values between sectors of the same size, each considered as homogeneously deformed. The importance of the scale effect and the difficulty of distinguishing between continuous and discontinuous deformation, are also emphasized. This study shows that the boundary shape of heterogeneities is an important factor in determining the appearance and the orientation of various structures; this is true for heterogeneities present before deformation as well as those acquired during deformation. The problem is still more complex because the heterogeneities (included folds) undergo a rotation during progressive deformation.

This study leads to models which may explain different associations of structures. For example, in any outcrop containing two layers of different competence: one layer is found with a fold axis parallel to the X lineation and the other one with the fold axis perpendicular to the same X direction. Other models allow an explanation for the successive appearance of various structures, such as folds of variable symmetry in a progressive non-coaxial deformation, or, in the same system, the evolution of cleavage planes.

GENERAL GEOLOGICAL SITUATION

The external crystalline massifs of the French Alps (Fig. 1A), composed of gneisses and granites (partly Hercynian in age), are covered by Mesozoïc sediments, deposited on a pre-Triassic peneplain. The cover begins with a thin Triassic sequence comprising sandstones and limestones (more or less dolomitic) as well as some basal volcanic flows and sills (spilites) and, locally, gypsum; it then continues with a thick monotonous series of black limestones and shales (Liassic—Upper Jurassic, locally Cretaceous). This series is nearly everywhere represented by regular alternations of more or less argillaceous limestones, in layers rarely up to half a meter in thickness.

In the Alpine orogeny all these rocks (including the basement) have been affected by successive phases of deformation whose characteristics vary according to the mechanical behaviour of the materials, their relative position and the geometry of the basement under the sedimentary cover.

The basement reacted by fracturing into large blocks which slipped against each other and which in places pinched their sedimentary cover into narrow

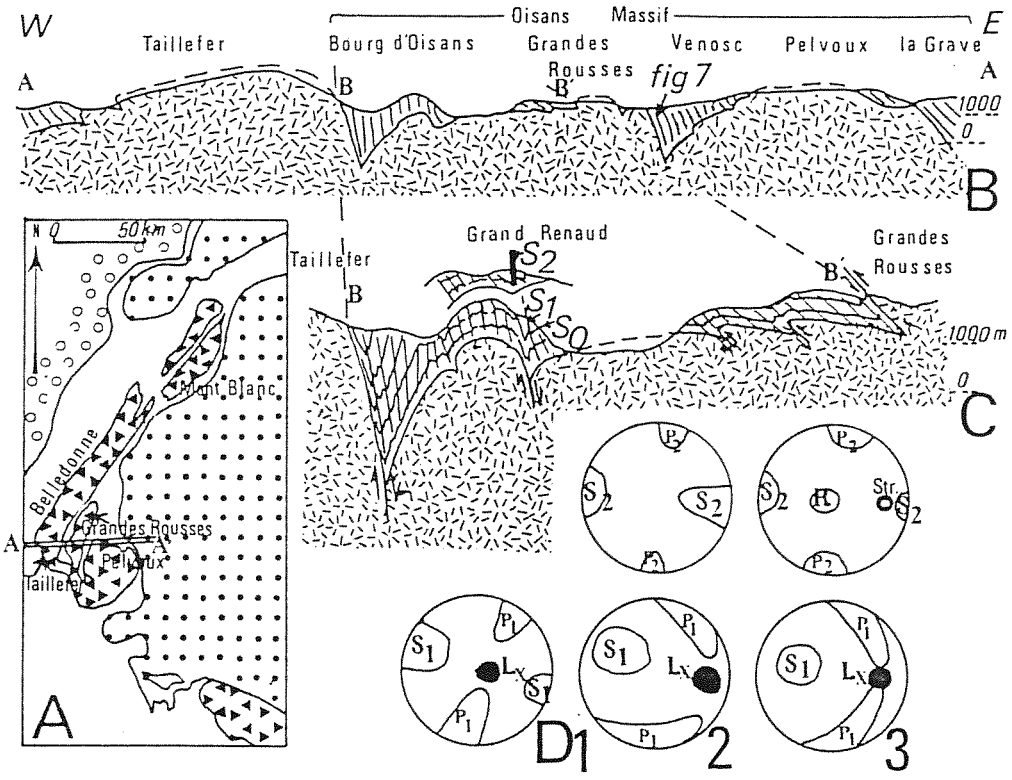

Fig. 1. A. General geological setting. Triangles = basement; dotted = internal zone (nappes); white = Mesozoic autochthonous sediments; open circles = Cenozoic sediments. B. Schematic cross-section (E—W) showing the shape of the basement-cover boundary with pinched synclines and wide anticlines. C. Magnified cross-section of Bourg d'Oisans (B.O.) syncline. S_0 = stratification; S_1 = slaty cleavage; S_2 = crenulation cleavage. Thrust plan in the eastern part, fault parallel to Alpine cleavage in basement in the western part. D. Stereograms (lower hemisphere) showing the relations between these structures: S_1 and P_1; S_2 and P_2; L_x = stretching and slipping lineations; R = overprinted S_1 fractures; *Str.* = striaes on R. D_1. Western and central part of the B.O. syncline. S_1 vertical, no S_2. D_2. Eastern part of the B.O. syncline. S_1 inclined. S_2 and P_2. D_3. Eastern part of the Grandes Rousses massif: S_1 inclined and S_2 and R.

"synclines". Certain masses of this basement also have indented, horizontally or vertically, the sedimentary series (Gratier et al., 1973; Boudon, 1976). Thus, the sedimentary series often subsided relatively to the basement, which now forms the mountain summits (Fig. 1B).

The Alpine faults of the basement, which may be old dislocations rejuvenated, have sometimes induced deformation in crystalline rocks whose last cleavages are certainly Alpine, as is demonstrated by their continuity and their association with the covering sediments. In these deformations, the main discontinuity (décollement) between the basement and the sediments is

not generally placed at the bottom of the Triassic. Thus the basal Triassic formations are most often competent and generally have reacted as an integral part of the basement. It is in the first calcareo-argillaceous levels of the top of the Triassic—Lower Jurassic, that the limit of the behavioural differences between the basement (with its adhering Triassic) and the cover, can be found. However, this rule is not absolute and in some cases the Triassic may be completely crushed: in such a case, the Liassic is in direct contact with the crystalline basement and is represented by densely cleaved argillaceous limestones or by discontinuous levels of cargneules and gypsum. This situation is perhaps related to a sporadic sedimentation of evaporites which are not always present in the Triassic.

The well-stratified monotonous argillaceous limestones of the Jurassic, are the formations which contain the most spectacular and representative structures due to deformation of the sedimentary cover. They include folds whose disposition is related to the shape of the basement masses: these enclose narrow "synclines" pinched between wider "anticlines" of basement (Fig. 1B, C).

The large P_1 folds are generally accompanied by a regionally well-developed axial plane cleavage (S_1), very often overprinted by a second crenulation cleavage (S_2). For west to east, across the succession of major "synclines" and "anticlines", there is a variation in the dip of the S_1 cleavage and of the associated axial planes of minor P_1 folds. Each "syncline" of the cover contains several real folds of sedimentary material. In the western part of the area these folds are most often upright and tend to be pinched between blocks of basement. Further east, they are progressively inclined towards the west: similarly S_1 passes progressively from the vertical, to eastward dipping, and then nearly horizontal (Fig. 1B, C).

In the eastern borders of the Grandes Rousses and Pelvoux crystalline massifs, in the direction of the Briançonnais nappes, S_1 passes from a strong vertical dip near the basement to a near horizontal dip under the bottom of the nappes, or at least, to an orientation parallel with this boundary (Fig. 1B).

USE OF STRAIN MARKERS

Strain has generally been estimated by taking the mean of values obtained using different methods only for local comparisons.

Description

Various structures were observed and described at different scales:

(1) In thin sections, for cleavages and fibrous crystals, in veins and pressure shadows.

(2) On outcrops, for all the planar and linear features measured with a compass. A relative chronology of these features was attempted.

(3) On photographs of high cliffs, perpendicular to the axis of large P_1 folds. After corrections, for distortion and scale effect, this allows the construction of true sections and exact shapes of these folds (see Fig. 2).

Determination of finite strain

Deformed fossils and folded veins have been used (see Fig. 9):

(1) Elongation values $\sqrt{\lambda_x}$ and $\sqrt{\lambda_y}$ were determined using truncated belemnites by the method developed by Badoux (1963) and Masson (1971) (see Fig. 10).

(2) The ratio X/Y is given for deformed ammonites and elliptical oxidation spots.

(3) The contraction values $\sqrt{\lambda_z}$ were estimated by the unrolling of ptygmatic folded veins (parallel to the stratification S_0) at the hinge of large P_1 folds. (It is a minimum value since these veins may also have thickened).

The exact shape of large P_1 folds is also used to calculate comparative values of contraction between several different sections (see Figs. 2 and 9):

(4) The apparent value of contraction perpendicular to the fold axis is estimated taking the arc length L_0 of the layer, as measured with a curvimeter on sections with correction for plunge axis, and the span L_1 of the fold along a direction perpendicular to the axial plan. It is only a comparative value because such a fold cannot simply be unrolled (the layers are cleaved).

(5) The ratio X/Y is also measured using the variation of the interlimb angle of the folds, with respect to a reference value obtained at the La Paute section (on sections with correction of plunge axis). This is also a comparative value, because the length of limbs is not constant during deformation.

The plunge of folds axis P_1, has also been measured and compared with all the strain estimates (see Figs. 9 and 10).

Evidence and measure of slip

The rocks generally exhibit evidence of deformation by slip on discontinuities and by penetrative shearing. Often the slip and shear are difficult to distinguish. However, when many striaes on bedding (S_0), cleavage (S_1 or S_2), or fractures, groove these different planes, the slip displacement is clear. On the limbs of a fold, the slip between adjacent microlithons (bounded by S_1 planes) adds to the internal deformation. Comparative values which integrate slip and strain have been estimated by the method shown in Fig. 3F (Vialon et al., 1976). This gives values of elongation parallel to the limb of folds.

The displacement of reference marks from point to point along planes of discontinuity has been only used when striaes are found on this plane (often on quartz or calcite infilling) because pressure solution may produce an apparent displacement of initial markers, without there being true slip on the plane.

Physical and chemical conditions of the deformation

Changes in chemical composition during progressive deformation of Liassic argillaceous limestones have been studied by chemical analysis (microprobe; or X.R.F., Gratier, 1979). Attention was focussed on hard objects (fossils, folded veins, etc.) which induced locally heterogeneous strains in an initially homogeneous matrix (see Figs. 11 and 12). Mobile minerals (SiO_2, $CaCO_3$, ...) have been shown to migrate from a solution surface (cleavage) to dilated zones (perpendicular fractures) where they crystallize. By comparing chemical analyses from differently deformed zones, quantitative measures have been made of this transfer process. Microprobe analysis, along sections perpendicular to solution plane, yield concentration profiles of various elements (see Fig. 11).

A study of fluid inclusions in various synkinematic veins infilled by mobile elements, has given the relation between temperature, pressure and nature of fluids (Gratier et al., 1973; Bernard et al., 1977, Bernard, 1978). The temperature of homogeneization of the fluid has been determined by heating the sample under the microscope. This leads to a minimum value for the crystallization temperature. If there was no volume change of the inclusion, it gives a density and an isochore (*P-T* relations). To determine the true pressure value, the true temperature of sealing is estimated by measuring the K/Na ratio in the fluid (Poty et al., 1974).

RESULTS

The tectonic structures and finite strains will be described separately for sectors (1) with upright folds (vertical S_1) and (2) with inclined folds (inclined S_1). In these two cases no difference exists for physical and chemical conditions of the deformation.

Structural description

Sectors with upright folds P_1 (vertical S_1)

The reconstructed sections of the Bourg-d'Oisans major "syncline" (between the basement of Belledonne—Taillefer and Pelvoux—Grandes Rousses) show, in the central and western parts of the "syncline", a system of upright folds more or less narrowly pinched between masses of basement; the shape of the folds varies from south to north according to the shapes of the basement and to the width available between crystalline masses. This width appears to have controlled the amplitude, wavelength, and frequency of minor folds (whose axes are mainly N—S but are moulded around basement blocks). In any given cross-section, the major "syncline" widens upwards and the minor folds display a decrease of E—W horizontal contraction value with the altitude. The shape of folds varies also, according to the distance from the basement (La Paute—Oulles cross-section) and between one section and another (Fig. 2).

Each minor domain is composed of alternating folds of class IC (competent levels) and class 3 (incompetent layers). In bulk, this combination gives similar folds (class 2) with often rather sharp hinges and straight limbs.

The detailed structures, quite homogeneously distributed throughout the whole "syncline", are spectacularly well exposed along the road which runs from the Lignarre valley to Oulles, a little village to the west of Bourg d'Oisans (Gratier and Vialon, 1975).

(a) *Slaty cleavage* S_1, which is vertical and roughly N—S, bears two lineations. One is the trace of bedding (S_0) enhanced by refraction of S_1 when it passes progressively from a calcareous to a more argillaceous layer. This S_0/S_1 intersection runs parallel to the axes of minor folds in the sector. It plunges either towards the north or towards the south: the plunge varies according to the different transverse cross-section of the syncline (see further on) but also varies between one S_1 plane and another at the same outcrop. In places one can observe on a single S_1 plane a curved intersection lineation which emphasizes this plunge variation (Fig. 3A).

The other lineation is regularly vertical: it is a preferred mineral orientation and the rock has a fibrous texture. It is also expressed by fine alignments of grains of oxidized pyrite, prolonged by crystallized fibres of calcite, quartz or gypsum (pressure shadows). It is a stretching direction parallel to the principal elongation direction X, as indicated by truncated belemnites and other deformed objects (oxidized spots, ammonites . . .). The stretching lineation is sometimes emphasized by striaes parallel to X.

There is a system of joints perpendicular to S_1 and parallel to X. This joint planes (longrain) often bear horizontal striaes.

The S_1 cleavage is cut also by subhorizontal fractures with infillings of quartz and calcite, often as drusy crystals whose long axes are parallel to the stretching lineation. In the more argillaceous beds these fissures are generally barren. We attribute these fissures to vertical stretching of the rock. The S_0/S_1 lineation, owing to plunge variations, is only rarely perpendicular to the stretching and this leads to some peculiarities in the organization of the horizontal fractures. The latter are often disposed en echelon (in an array orientated by the S_0/S_1 lines) which expresses an apparent rotation in the S_1 plane. This shearing also entails the disjunction of each fracture into elementary segments which correspond to Riedel fractures (Fig. 3B).

(b) *Perpendicularly to the* S_1 *plane*, the refraction of the cleavage can be easily observed: in the most argillaceous layers, S_1 is nearly parallel to S_0; in the more calcareous levels it subtends a larger angle (Fig. 3E).

The strata form sigmoïdal "microlithons" whose relative position and apparent displacements are distributed normally across the folds. This intermicrolithon slip (and associated shear) is parallel to the stretching lineation. It can be measured (Fig. 3F) and gives an estimate of the local elongation parallel to the fold limbs. It is an element of comparison between structures,

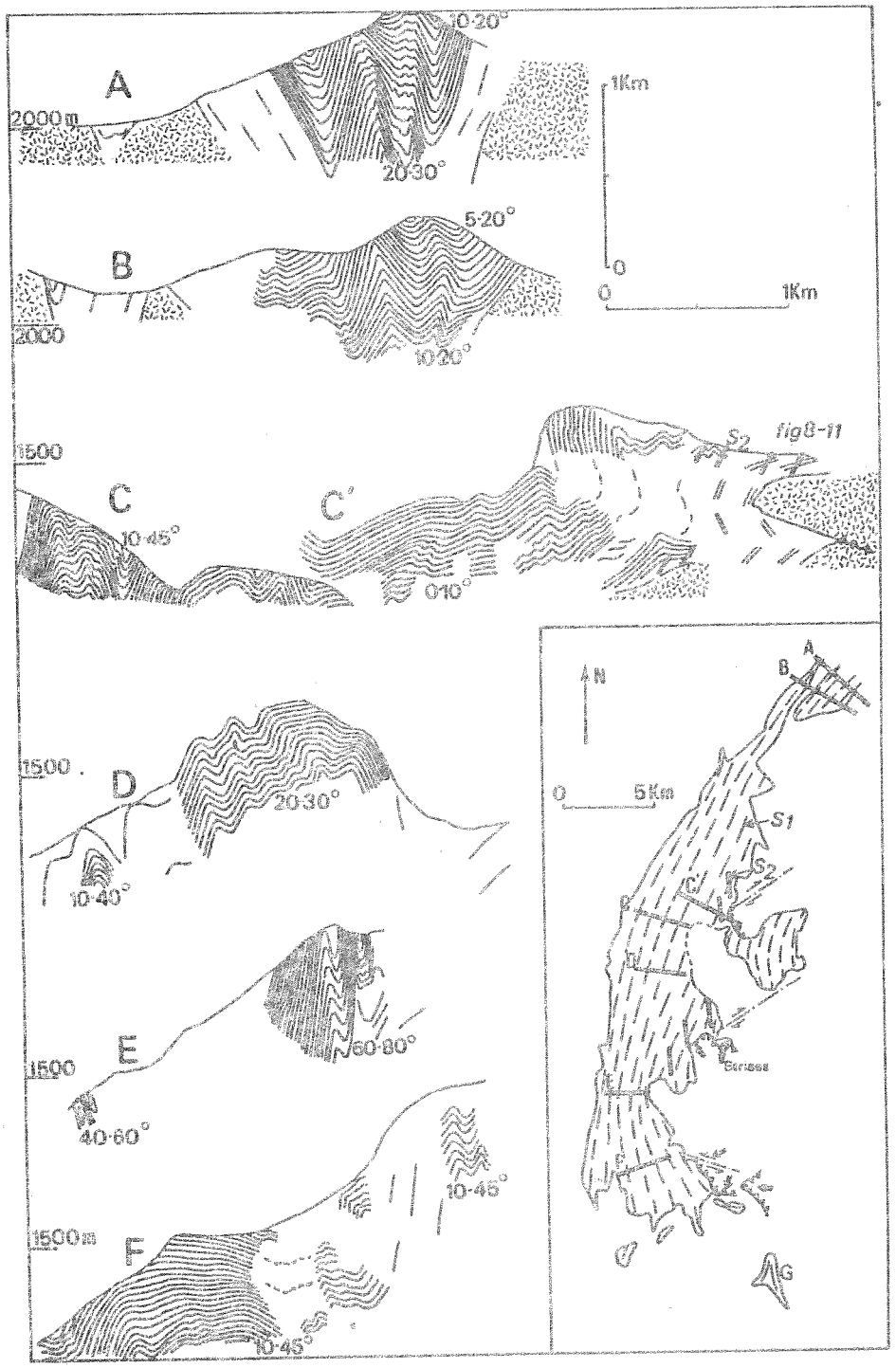
A
2000 m
0-20°
20-30°
1Km
0
0
1Km
B
2000
5-20°
10-20°
1500
C
10-45°
C'
0-10°
S2
fig8-11
1500
D
20-30°
10-40°
E
1500
50-80°
40-60°
1500m
F
10-45°
10-45°
N
0
5Km
A
B
S1
S2
Carisbrook
G

which will be used concurrently with the elongation ratios measured by other means.

In this intermicrolithon displacement of the competent calcareous layers, owing to the refraction and the sigmoïdal shape of these objects, an interlocking defect appears with filling of various minerals (Fig. 3C). The resulting veins are filled with fibrous calcite and quartz crystals whose sigmoïdal disposition confirms the direction of the displacement. Subsequent phases of vertical stretching have caused boudinage of these intermicrolithon fillings. The boudins axes are crossed so as to define lozenge-shaped boudins. The axes correspond to an interference between the directions parallel to the fold axis (S_0/S_1) (which are progressively more and more plunging in the progressive deformation) and the direction perpendicular to the vertical stretching (Fig. 3G).

Because of the rotation of the contraction direction during the progressive deformation in the limb of fold, the present cleavage is sometimes oblique to the initial cleavage represented by the boudinaged intermicrolithon veins. In such a case the final cleavage dissolves the quartz-calcite filling (Fig. 3D). But in general when these microlithons have been slipped and sheared, in the limbs of the fold, the present cleavage in the competent layers remains subparallel to the boudinaged intermicrolithon filling (Fig. 3E).

(c) *When the S_1 cleavage is parallel to the S_0 bedding*, certain layers are extremely boudinaged. Two cases are met with. In the first, the layer is thin (10 cm) and the boudinage is expressed by quartz and calcite fillings between segments of the truncated layer: subsequently the fillings have resisted to the deformation and the residual segments have been thinned and stretched. This "boudinage of boudins" seems to develop during one progressive deformation.

The second case of boudinage shows the complete disappearance, over several dozen meter of a layer, without any recrystallization between disjuncted sections. The boudinaged layer thins out, becomes highly cleaved and disappears, leaving a single plane analogous to the mingled S_0—S_1 planes which separate two normal layers.

The strong vertical stretching is also revealed by veins predating the cleav-

---

Fig. 2. True sections, reconstructed from photographs of vertical cliffs (with correction for distortion and different scale effects). Section perpendicular to the axial plane of P_1 (S_1 cleavage) displaying the variation of the fold shape from north to south, and relative to altitude and distance from the basement. The average plunge of fold axes is indicated. The position of each section is shown on the map, where the direction of S_1 cleavage is also indicated (dashed) to show the indentation of the cover by the horizontal movement of the Rochail basement massif. S_2 cleavage (thick dashed) limited to a N50 sinistral zone and thrusting of basement over cover (toward north and south) are also associated with this indentation (white = basement). A. Aiguillettes Nord. B. Aiguillettes Sud. C. Oulles. C'. La Paute. D. La Lignare. E. La Malsanne. F. Le Tourot. G. Côte Belle.

The Rochail massif is at the eastern end of the "E" section.

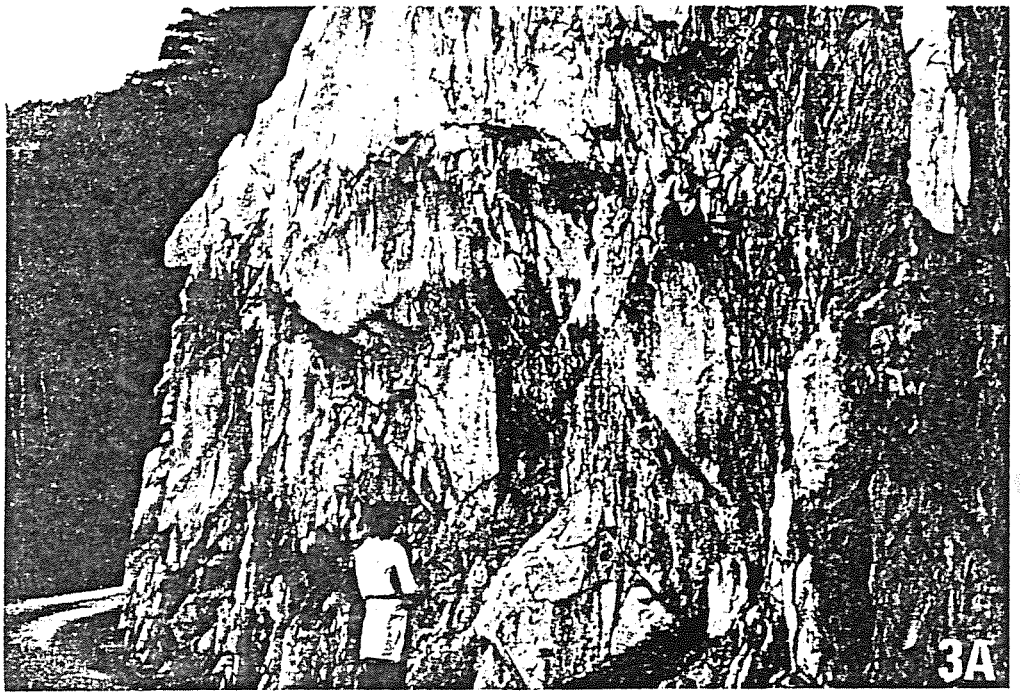

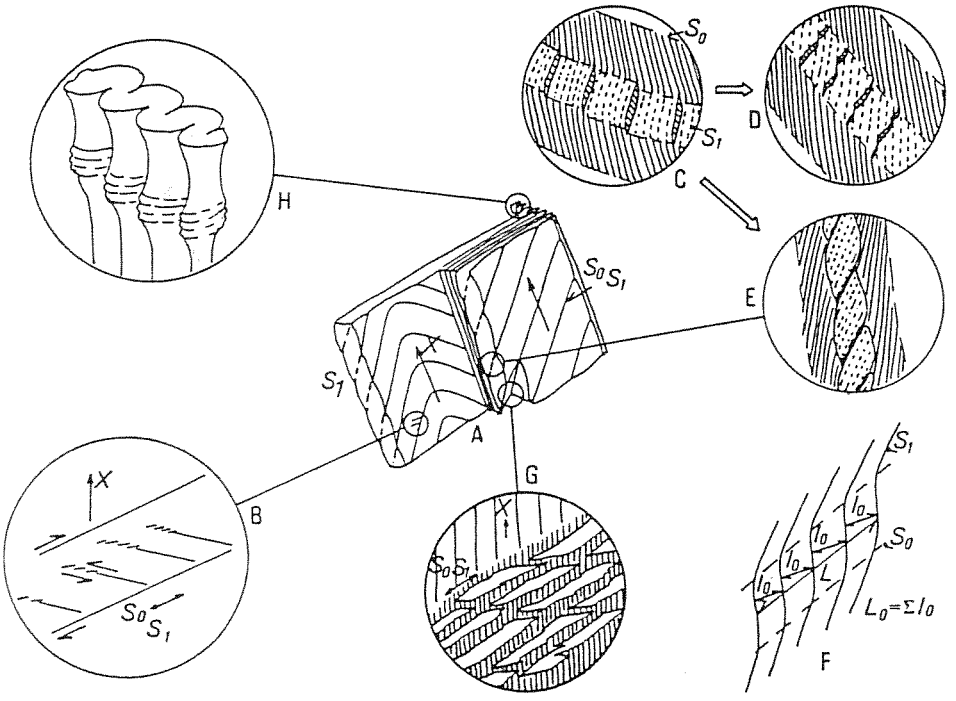

Fig. 3. A. Arch of S_0/S_1 intersection lineation (parallel to the fold axis P_1) on one cleavage plane S_1. Different plunge for different S_1 planes. B. Subhorizontal en echelon fissures on the cleavage plane. Disjunction of each fissure into small Riedel fractures. C. Elongation and movement parallel to S_1 producing dilatation in competent layer, with infilling of intermicrolithon (interlocking defects). D. Penetrative cleavage oblique to the boudinaged intermicrolithons filling in a competent layer owing to the rotation of the contraction direction during progressive deformation (S cleavage always perpendicular to

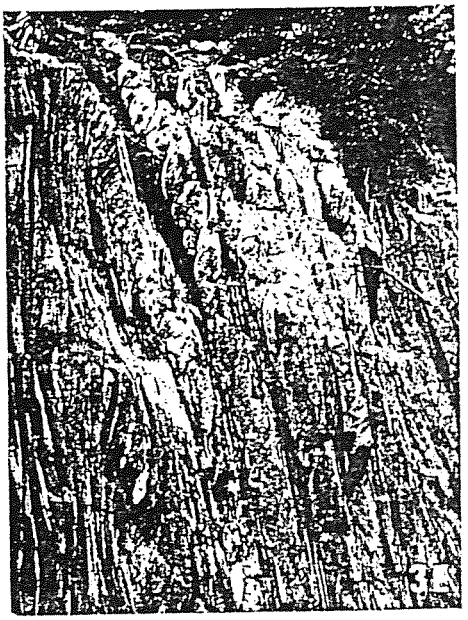

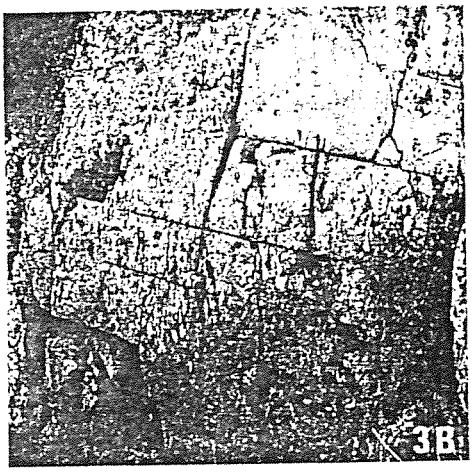

Z direction). E. Penetrative cleavage parallel to the boudinaged intermicrolithon filling in a competent layer, shearing and slipping parallel to the S plane, with rotation of the contraction direction. F. Measurement of shear and slip of microlithons in fold limb. G. View of S_1 plane boudinaged intermicrolithons filling with two boudin directions: one parallel to reorientated fold axis, the second perpendicular to the constant X direction. H. Bamboo stalks. Double boudins of a ptygmatic fold hinge of a previously vertical calcitic vein perpendicular to S_1.

age. Originally, these veins were probably vertical and normal to the initial S_1 plane (i.e. perpendicular to the initial fold axis). With the development of S_1, the veins have been folded ptygmatically with vertical axes. The resultant stretching is now parallel to these fold axes. Their hinges are boudinaged according to the same two-stage processes above described: this "boudinage of boudins" has produced grooved bodies comparable to bamboo stalks (Fig. 3H).

Sectors with inclined folds P_1 (inclined S_1)

On the eastern side of the Bourg d'Oisans syncline (Fig. 1B, C) the observable P_1 folds are inclined and symmetrical but they are located in a hinge zone of a larger fold (stratigraphically inferred) which is probably asymmetric (Fig. 1C). The various directions of P_1 folds are indicated in Fig. $1D_2$.

On the eastern side of the Grandes Rousses massif, asymmetric inclined folds are small (<1 m). Their axes are dispersed in all the directions in the S_1 plane (Fig. $1D_3$). Their vergence varies due to this dispersion. For example, from Mizoen to Singuigneret, the fold axes vary from N10 to N120 with an overturned limb toward the west and the south. These folds may be minor folds on a larger fold, but in all the sector, the relations between slaty cleavage and bedding almost always indicate normal limbs. Overturned limb relations are rare. The spatial distributions of folds is not well exposed in the cover of the Oisans massif, but we have found very similar structures throughout the sedimentary cover of the external basement massifs. For example, the photograph (Fig. 4) taken in the region of Mégève (cover of Mont-Blanc massif) shows the folded zone limited by two horizontal layers (with many striaes parallel to the X direction). The dip of the axial plan decrease from the upper and lower limit of this folded zone to the central part. The amplification of fold increases according to this decrease of axial plane dip. In this folded zone we often found a thrust fault limited to one or two layers.

In the sector of inclined S_1 the strain markers are often similar to those previously described. But they are simply tilted by 30° to 60°, as the S_1 plane (Vialon, 1968).

The stretching lineation (average trend E—W but ranging from N60 to N140 near the basement) is a preferred mineral orientation, which is parallel to the long axes of ellipsoidal objects (ammonites-oxidation spots). On a section perpendicular to S_1, pressure shadows are frequently asymmetric. They mark a component of shearing parallel to the S_1 plane. In contrast to the preceeding sector, an inverse sense of shear in the two limbs of a fold may be observed but only in slightly flattened folds. For strongly flattened (amplified and inclined) folds, the sense of shearing is the same for the two limbs, with displacement of the upper part toward the west (Fig. 5). Many striaes on planes of discontinuity (S_0, S_1, fractures) mark this same direction of displacement. These striaes are parallel to the stretching lineation (Fig. 6). Sometimes early striaes on S_0 plane are unrolled by ptygmatic folds P_1.

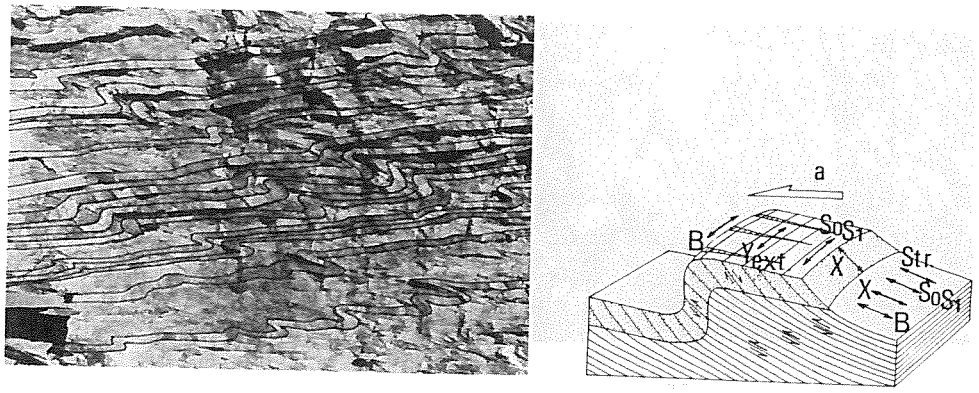

Fig. 4. Spatial distribution of asymmetrical inclined folds P_1 with axial cleavage S_1. The axial plane of the most amplified folds tends to become parallel to the horizontal strata in a central part of a foldband. This may be linked to a shear zone parallel to the strata.

Fig. 5. Relation between fold axis B, S_0/S_1 lineation, slip lineation, stretch lineation, and direction of shear ("a"). (1) In a competent layer: S_0/S_1 (B) parallel to Y (minimal elongation), perpendicular to X (stretch and slip lineation) and to (a) direction. Different sense of movement on cleavage for normal and overturned limb. (2) In an incompetent layer: S_0/S_1 (B) parallel to X (stretch and slip) and almost to (a) direction. Same sense of movement on cleavage for normal and overturned limb (sense of general shearing).

The S_0/S_1 intersections (or P_1 fold axis) are frequently curved on the S_1 plane (Fig. 6). In folds affecting more competent rocks (which are less flattened, less amplified, and almost perpendicular to the X direction), we have noted an elongation marked by pressure shadows parallel to the fold axis. We also found this elongation along the Y axis, with truncated belemnites (Fig. 10). Figure 5 outlines the relation between the different lineations in a competent and an incompetent layer (see also Hansen, 1971; Brun, 1978).

Two other structures are characteristic of this sector with inclined S_1: a crenulation cleavage (S_2) and subhorizontal fractures overprinting S_1 (Fig. 7). The S_2 crenulation cleavage is a pressure-solution cleavage (Fig. 11) which obliterates S_1 in the more incompetent layers (Fig. 8). The angle between S_2 and S_1 is never less than 30°. (If the contraction direction is greater than 60° from S_1, the dissolution probably occurs on S_1). The S_2 cleavage is mostly vertical with a N—S trend (Fig. 1D$_3$). Nevertheless, near the basement or near heterogeneities which are included in the sedimentary cover (fossils, folded veins, etc.) the S_2 plane is parallel to the boundaries of the most competent parts (Figs. 1D$_2$ and 2). Thus several directions of S_2 may appear on the same outcrop.

In the east of the Grandes Rousses and at low altitude in the Bourg d'Oisans syncline (1000 m), where S_2 is limited to the incompetent layers, the amount of shortening normal to S_2 is small with respect to that associated with S_1. But at higher altitude (from 2000 m to 3000 m) in the Bourg

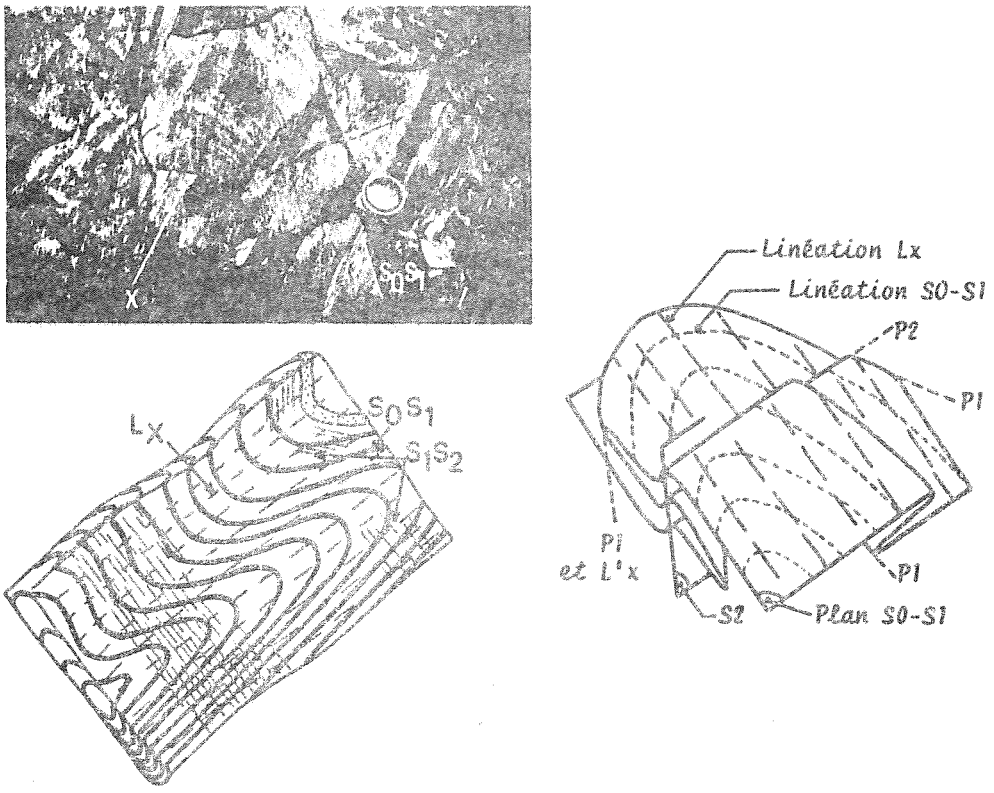

Fig. 6. Different lineations on S_1 planes: X stretching (internal strain) and slipping (striae) lineation. S_0/S_1 intersection parallel to P_1 axis. With small elongation (Y) when P_1 is perpendicular to X. S_1/S_2 lineation: crenulation cleavage locally moulded on S_0/S_1 heterogeneity.

d'Oisans syncline large P_2 folds (10—100 m) appear, which implies a more important horizontal E—W contraction (Fig. 1C, section of the Grand Renaud).

The second characteristic structure begins by wide waves of S_1, giving almond shapes (Fig. 7). When the waves are magnified, the planes of S_1 coalesce and there ensues a rupture: horizontal fractures crossing S_1 are expressed. This plane (often infilled with calcite and silica) on which striaes show the relative slip always parallel to the slip-stretch lineations on S_1 (Fig. 1D), always stands at an angle of about (20—30°) to S_1.

Finite strain values

Sector with upright P_1 folds (vertical S_1)

Most of the comparative values of the finite strain estimated by different methods (above described) are gathered in the table Fig. 9. They are all con-

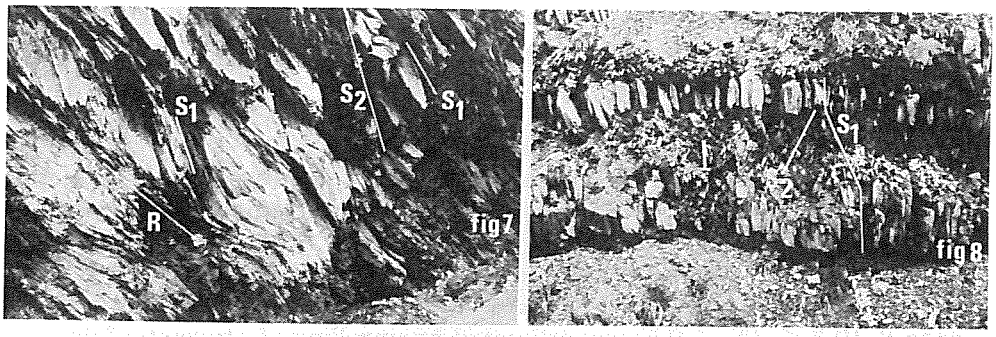

Fig. 7. The two characteristics structures of sectors with inclined P_1S_1: S_2 crenulation cleavage and R fracture overprinting S_1, with striae (on the R infilling of calcite and quartz). See Fig. $1D_3$. Situation on Fig. 1B.

Fig. 8. Refraction of S_1 cleavage and S_2 cleavage in incompetent layer. Situation on Fig. 2, section C′.

nected with the different transverse sections (Fig. 2). For some of these sections, there are several values, according to the different altitudes, and to the horizontal distance to the Taillefer basement massif, and to the width between the two basement boundaries. The value of the plunge of the P_1 fold axis which is also plotted, may be matched with these different strain

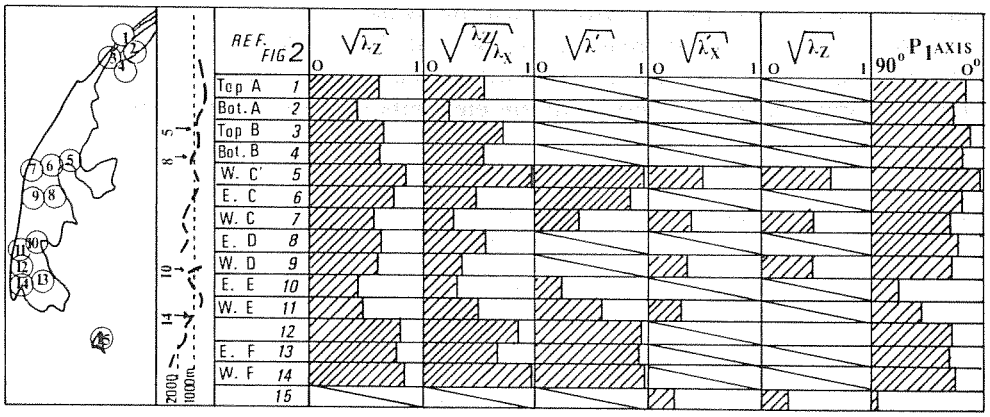

Fig. 9. Table of comparative strain values in Bourg d'Oisans syncline: 1st and 2nd rows: situation of measures (*1*) on schematic map, (*2*) on a longitudinal section of B.O. Several values are given for each sections, according to position (altitude, distance from the basement). 3rd row: see Fig. 2. 4th row: apparent contraction on a section perpendicular to the axis of the fold (with correction for plunge of fold axis). 5th row: contraction measured by the angle between fold limb (reference to the fold of La Paute, with correction for plunge of fold axis). 6th row: values of the intermicrolithon slip and shear in cleaved competent layer (reference to the fold of La Paute). 7th row: elongation of truncated belemnites. 8th row: apparent contraction in a section perpendicular to the interstratified calcite veins (at the hinge of P_1 folds). 9th row: values of the plunge of P_1 fold axis.

values. It increases with the increasing of the ratios X/Z and X/Y. The diagrams using truncated belemnites are given to allow a discussion on the significance of these elongation values (Fig. 10).

Sector with inclined folds (inclined S_1)

For this sector we have obtained fewer well distributed measurements than in the preceding sector. The truncated belemnites have given values of $\sqrt{\lambda_x}$ ranging from 1.6 to 3.2, with an average of 1.9. Most of the values of $\sqrt{\lambda_y}$ are 1. The ammonites and the oxidation spots have given a X/Y ratio ranging from 1.3 to 2.2, with an average of 1.8. The shortening perpendicular to S_1 ($0.3 < \sqrt{\lambda_z} < 0.5$) was estimated by unrolling of ptygmatic folds.

Physical and chemical conditions of deformation

Measurement of pressure solution

Although both cleavages are very different in their aspect (since the slaty cleavage (S_1) is penetrative whereas S_2 is a crenulation cleavage), they exhibit very beautiful examples of structures attributed to pressure solution (Figs. 11 and 12). This interpretation is supported by chemical analyses (Gratier, 1979). For example, the distribution of various elements (Fig. 11) obtained by electron microprobe scan, shows that the cleavage plane is a zone of depletion in Ca and Si and of relative increase in Al, Mg, K, Fe, Ti. An XR analysis gave the mineral content, the same minerals appear in the cleaved and non-cleaved rocks but with a clear decrease in content of calcite, quartz and dolomite, and an increase in content of illite (2 M), chlorite, pyrite, in the cleavage plane. Assuming that this increase of insoluble minerals is due only to solution of the most mobile elements (calcite, quartz, etc.), a con-

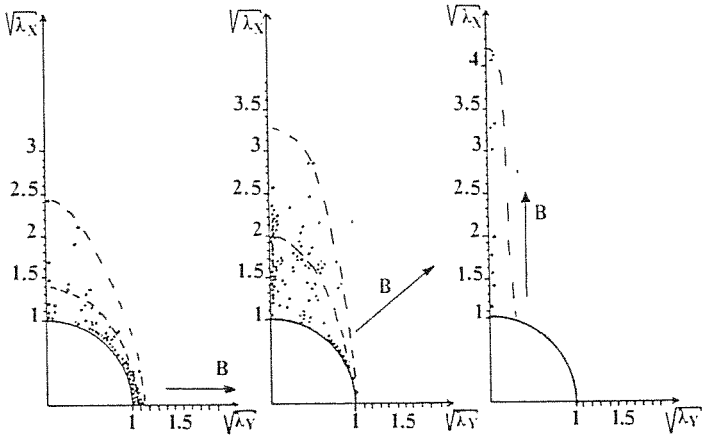

Fig. 10. Diagrams of truncated belemnites. The arrows show the plunge of P_1 folds nearby.

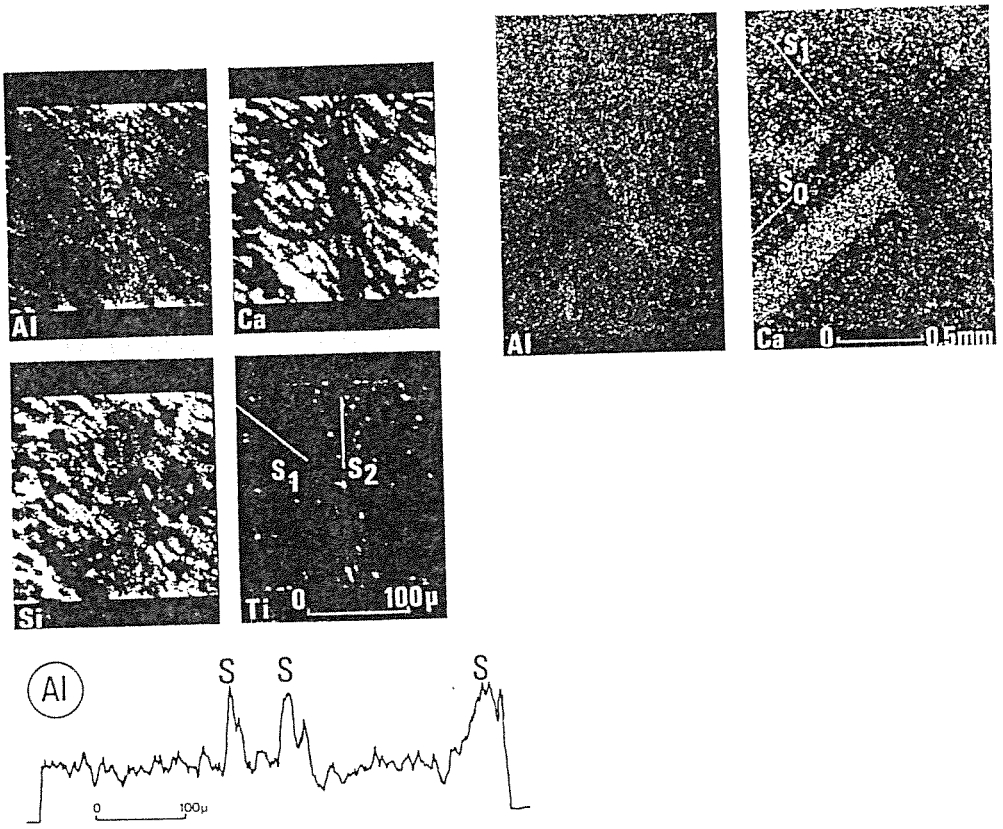

Fig. 11. Chemical distribution of various elements across a cleaved rock. A. Distribution map of Al, Ca, Ti, Si (electron microprobe scan CAMECA MS 46). Crenulation cleavage S_2 (central part) overprinting a slaty cleavage S_1. B. Distribution map of Al and Ca (electron scan with XR analysis). Calcareous hard objects lay down parallel to S_0 strata, with solution plan cleavage S_1 sub perpendicular. C. Integration of the Al content, on a 200 μ width profile perpendicular to S_2 (automatic scanning (200 μ) parallel to S_2 and displacement of the sample perpendicular to this S_2 plan).

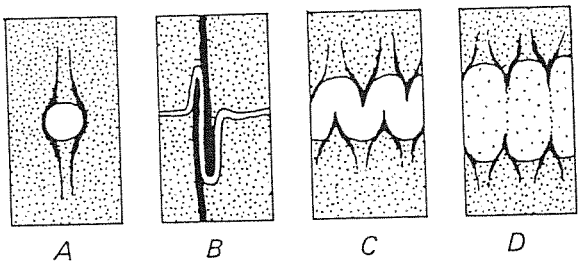

Fig. 12. Pressure solution plane associated with heterogeneities: (A) around a hard object; (B) at the level of a vertical limb of fold; (C) in the intrados of a ptygmatic fold, affecting a whole layer, (D) affecting only the upper and the lower limit. Insoluble elements in black.

traction value has been estimated for the cleaved zone. For example, normal to S_2 profiles, obtained with microprobe analysis, allow one to calculate a shortening perpendicular to S_2 of 17% (Gratier, 1979). An elongation, perpendicular to this contraction, appears, due to the crystallization of the mobile elements. But this elongation is at various scales, according as the mobile elements migrate far from the cleavage plane (toward dispersed tension gashes), or the mobile elements remain near the solution plane, by recrystallization around mineral grains. (These recrystallizations are revealed by studies of cathodoluminescence on thin polished sections).

Temperature and pressure of deformation

In the sedimentary cover, the temperature of homogeneization (or the density) decreases with distance from the basement (Fig. 13A). The contours of equal temperature are roughly parallel to the basement cover boundary. The histograms spread out because of the grouping of inclusions from veins of different ages. A decrease has been also observed from the earliest vein (ante-S_1) to the latest (post-S_1) (Fig. 13B). Even after this differentiation the value remains scattered due to successive generations of inclusions in the same crystal.

A true temperature has been estimated (K/Na ratio) for the post-S_1 vein, only in the basement (lack of feldspar in the cover veins). They vary ranging from 335°C to 370°C (Poty et al., 1974) at the basement cover limit. This

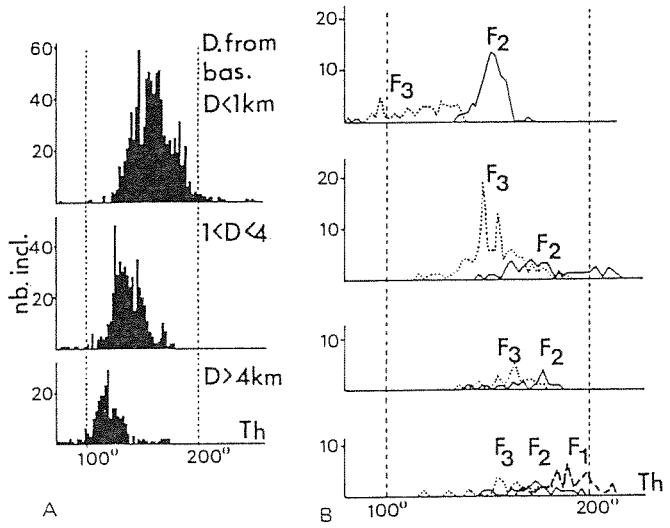

Fig. 13. Study of fluid inclusions. Distribution of the homogeneized temperature of various synkinematics veins in the cover: A. According to distance from the basement (grouping all the veins). B. According to age of veins — F_1 ante S_1 (parallel to S_0); F_2 syn S_1 (filling of S_1 in competent layer and en echelon associated veins); F_3 post S_1 (associated with S_2 cleavage and R fractures).

implies a pressure ranging from 200 mPa to 250 MPa (Bernard et al., 1977).

The fluid in the inclusions is water with a small NaCl content, decreasing with distance from the basement.

INTERPRETATIONS

General problems

Values of finite strain and volume change

On the diagram of Fig. 10, the elongation values of truncated belemnites vary for a given angle with the stretching lineation (X). Two explanations are possible and are not incompatible: (1) The difference in competence between fossils and matrix varies for a homogeneous deformation. (2) The deformation is inhomogeneous.

In the first case the best estimate of the elongation is given by the most elongated belemnites. In the second case we may take only a certain average of these elongation values. When comparing these values with those given by the ammonites and the oxidation spots (also minimum values) we notice that the latter give values lower than the most elongated belemnites but very close to the average value of this elongation. Using this last value and the contraction value given by the ptygmatic fold, a volume change could be estimated. On the example from La Paute: $\sqrt{\lambda_z} = 0.6, \sqrt{\lambda_x} = 1.4, \sqrt{\lambda_y} = 1.05$, the volume decrease is 12%. Taking the most elongated belemnites, we find an increase of volume which seem unreasonable. But the value $\sqrt{\lambda_z}$ is also a minimum value, since the vein may be thickened. The estimation of volume change using markers of competence different from the matrix, is thus doubtful in an heterogeneous material (Gratier, 1976).

Relation between strain values and plunge of fold axis (P_1)

The values outlined in the table Fig. 9 are only comparative, but they show a very good correlation between strain intensity and the variation of plunge of fold axis (P_1) (Gratier et al., 1976). This is also exhibited in the diagram of the truncated belemnites (Fig. 10). The greater the plunge is, the greater the X/Y and X/Z ratios are. Taking $\sqrt{\lambda_x}$ equal to the average value of elongated belemnites, for $\sqrt{\lambda_x} = 1.4$ the fold axis are subhorizontal, for $\sqrt{\lambda_x} = 1.9$ they plunge at 45°, for $\sqrt{\lambda_x} = 2.5$ their plunge reaches the vertical. Nevertheless, there is a problem. Assuming that the P_1 axes are (as a lineation) reoriented in the S_1 cleavage by increase of the deformation, the diagram of Ramsay (1967, p. 131) may be used. To pass from a gentle plunge of fold axis (10°) to a strong plunge (80°) the X/Y ratio must change from 1 to 0.03. The measured strain values do not show these variations. There are several possible reasons for this, for example:

(1) The greater the value of $\sqrt{\lambda_x}$, the more it is underestimated using truncated belemnites. This seems very unlikely.

(2) There is a contraction parallel to (Y) when the X/Y ratio increases. We

found no evidence for this, except in the sectors with fold axis parallel to X. We noticed very local and rare crenulation lineation parallel to X which marks a slight contraction normal to Y.

(3) The variously obtained strain values are too general: the deformation is inhomogeneous and so is the fold axis plunge (variable plunges on a S_1 plane and from plane to plane). If some cleavage planes show a very large value of X/Y ratio, this value cannot be seen when taking the measures over a large (100 m) outcrop. This last hypothesis is consistent with the observations: in the sector of Oulles, with fold limbs parallel to their axial plane, we have often seen some incompetent layers between two more competent layers becoming thinner and even completely disappearing over a dozen meter length. The fold axes are the most reoriented in this incompetent layer. This strongly elongated zone may evolve into a discontinuity plane on which slipping still contributes to the reorientation of fold axes. Only some of the S_0 or S_1 plane become sliding planes. It is also well-illustrated on the observed example of Fig. 5 (Plotto, 1977): this fold axis is completely reoriented and parallel to the X lineation in the incompetent level and it remains subperpendicular to this same X direction in the competent level. Consequently the role of the heterogeneity of the rock is important (see below).

Role of the heterogeneity of rocks

These rock heterogeneities may be prior to the deformation (difference between basement and cover, heterogeneous multilayered sediment, fossils, etc.) or acquired during progressive deformation (block of basement indenting cover, folding, boudinage, zone with depletion or deposition of mobile element). We particularly underline this last phenomenon which leads to a differentiated layering (Hobbs et al., 1975).

The planar and linear heterogeneities may be folded. Those with globular shape may indent the surrounding matrix. This appears on all scales from microscopic (see Fig. 12, hard object with associated parenthesis shape of solution plane) to macroscopic (see Fig. 2, the indentation of cover by a basement block). This indentation highlights some markers which would not otherwise appear so clearly.

The rotation of these heterogeneities (with increasing of the strain values) leads to a complex finite deformation, with fold axes or boudin axes oblique to the stretching lineation X. Another curious consequence of the heterogeneity is the infilling of some cleavage planes of competent layers (Fig. 3C). It may be explained by a movement along a refracted cleavage surface, producing a dilatation in the competent layers (Ramsay, 1967, p. 407). The high fluid pressure probably facilitates this phenomenon.

Evolution of cleavages in a non-coaxial deformation

There are different possibilities for the evolution of cleavages within a non-coaxially deformed zone (Autran et al., 1975; Choukroune Lagarde, 1977).

Assuming that the intermicrolithon filling plane in competent layers represents the initial cleavage, three different cases may be found in a limb of the fold (see also Le Corre, 1978).

(1) The actual penetrative cleavage plane crosses the intermicrolithon filling plane (with partial dissolution of this filling, Fig. 3D). Then, at every stage of non-co-axial deformation, the penetrative cleavage plane must be destroyed and reformed perpendicular to the contraction direction (Z) (S is always perpendicular to Z).

(2) The actual cleavage is parallel to the intermicrolithon filling plane (Fig. 3E). The initial cleavage plane remains the same all through the progressive deformation, but undergoes a rotation with shearing parallel to this plane (asymmetric pressure shadow within microlithon) and/or slipping on a particular plane (striaes on the filling at the limit of the microlithons). This case probably appears if the rate of cleavage process (pressure solution or any creep) cannot follow the rate of rotation of the direction of contraction (Z) as in the first case.

(3) The cleavage S_1 is overprinted by a later crenulation cleavage S_2 (Fig. 7). In such a case the rotation of the Z direction is presumably too fast to be registered as in the two former cases.

Fluids in the deformation

The presence of fluid (water with a small content of NaCl) probably facilitated the diffusion of the mobile elements.

The temperature evinced a clear thermal effect of the basement (Fig. 13A) (350° near the basement, 250° further on). It also decreases with the age of the vein (Fig. 13B).

The fluid pressure may be interpreted in two ways (Bernard et al., 1977):

(1) The fluid pressure is equal to the lithostatic pressure. Then for 200 MPa one must admit 7.5 km thickness of rocks. The actual thickness of known cover is only 2 km to the upper Cretaceous; so this implies that a great deal of material have disappeared (autochthonous sediment, nappes, water!).

(2) The fluid pressure differs from the lithostatic pressure, for example a transitory fluid overpressure may induce hydraulic fractures, with crystal growth when opening the fissure (decrease of pressure). The sealing pressure registered by the fluid inclusion is lower than the over-pressure but may be greater than the lithostatic pressure.

Sectorial interpretations

Sectors with upright P_1 folds (vertical S_1)

(a) Evolution of upright folding. The comparison between the central part and the western part of La Paute—Oulles section, allows us to build up a model of the fold evolution. We assume that the amplified fold of Oulles has

passed through a less amplified stage like those of La Paute. With an E–W continuous and horizontal contraction, the folds are initiated with vertical axial slaty cleavage, vertical stretching (thickening of layers) and slight elongation parallel to the horizontal fold axis (Y direction). Transfer of mobile elements (calcite, quartz) takes place by dissolution and recrystallization. Due to their refraction some cleavage planes in competent layers are infilled with these mobile elements. These fillings are boudinaged with increase of the E—W contraction, the axis of boudins is parallel to the fold axis.

Finally, all the axes begin to be oriented when the folds are amplified. The limbs become parallel to the axial plane and the axes (folds, boudins) become parallel to the vertical stretching direction. On account of the inhomogeneity of the deformation, the fold and boudin axes show various orientations in a single outcrop. The first boudin axes are parallel to the fold axes, the last ones are perpendicular to the X direction. The last crystallization takes place in large horizontal fissures. The slip direction on the different discontinuity planes remains parallel to the X direction during all the progressive deformation (see also Ayrton, 1972; Ayrton-Ramsay, 1974).

Spatial variation of the strain values. (1) *Variation of strain with altitude.* All along the Aiguillettes section (Figs. 2 and 9), the horizontal contraction value decreases from the bottom to the top, with a minimum value at the middle and increases with the inclination of the S_1 cleavage. On the top of the Aiguillettes the axial planes of folds converge toward the heart of the pinched syncline, like cleavage-fans in an ordinary incompetent layer. The basement-cover boundary forms (Fig. 1B) narrow synclines pinched between wider anticlines. This is similar to the folding of two materials of different viscosity (Ramsay, 1967, p. 383). The E—W contraction is maximal at the heart of the syncline, but along the basement-cover boundary, the contraction decreases and disappears in the sedimentary cover situated above the basement anticline (normal N—S fault which cuts out the cover and the basement in Grandes Rousses massif). In the basement, the whole deformation is concentrated in narrow strips near the pinched synclines.

(2) *Variations of strain values with horizontal E—W distance.* There is a good example on the La Paute and Oulles sections (Figs. 2 and 9). The greater amplitude of the folds in the western extremities of these sections (near the limit fault of the Belledonne Taillefer basement) is, perhaps, due to an heterogeneity of the sediments, on a transversal section of the Bourg d'Oisans syncline. But it may also be due to an early appearance of folds near the border of the deformed zone. This would be a boundary effect (see Cobbold, 1976). In this case, the first folds appear at the limits of the deformed zone and are therefore always more amplified than those which appear later at the center of the deformed zone. The thermal effect of basement may be also important. Moreover, there was a difference in anisotropy, acquired during deformation. In the central sector of the Bourg d'Oisans syncline, on the less contracted part, the two main planar features of the

material cross each other ($S_0 + S_1$, perpendicular or oblique up to a minimal angle of 50°), whereas at the western border the two planar features tend to be parallel. In the latter area, which is close to the basement border of the syncline, this arrangement facilitates the vertical elongation of the material, and therefore increases the vertical stretching—horizontal contraction relation.

This type of deformation is to be compared with the experimental deformation obtained on an orthotropic rock: under isotropic stress, the obtained strain can be represented by an ellipsoid whose small axis is perpendicular to the anisotropic plane of the material (Allirot and Boehler, 1976).

(3) *Variation of strain values with horizontal NS distance.* These variations are independent of those so far described, upon which they are superimposed. Proceeding from north to south, it is clear that the E—W horizontal contraction is very important to the north (Aiguillettes), decreases up to the sections of La Paute—Oulles, then increases as far as La Malsanne, where it reaches a maximum, before decreasing again as far as the Tourot section. This maximum of the Malsanne region also corresponds to the maximal curving of the syncline and of the axis of the regional folds.

We have been able to connect this arc with the horizontal indentation and rotational movement of the Rochail basement block, bounded by wrench faults (Fig. 2B). The S_2 cleavage localized near the wrench fault zone (trend N50°) at the north of the Rochail massif may be connected with this movement. The thrusting of basement over cover toward the north and south may be related with a deformation of the indentor. Other less spectacular indentations of cover by basement blocks exist to the north and south, and help to explain the local presence of a N—S horizontal elongation (parallel to Y).

Sectors with inclined fold P_1 (inclined S_1)

The characteristic structures of this sector are plotted on a stereographic projection (Fig. 1D). The poles of the S_2 cleavage, those of the fractures crossing S_1 (R), and those of the direction of striae on this plane, are all situated in a plane which also contains the stretching and slipping directions on the S_1 cleavage. Taking into account this fact and the evolution of the asymmetric P_1 folds (Fig. 4), we think that all these various structures may appear in a progressive non-co-axial deformation, with shearing parallel to the main fabric (stratification or cleavage), and variation of thickness of the shear zone. Many examples, not only in the Alps but also in the Himalaya and chiefly in the "Côte Basque" (western Pyrenees) have led us to propose three general cases (Gratier et al., 1978):

(1) In a shear zone parallel to an initial fabric (Fig. 14A_1) a local blocking of the movement may induce folding (A_2) (Rhodes and Gayer, 1977; Robert, 1979). This blocking (or at least a differential rate of displacement) may be due to an heterogeneity, or to a local thrust fault. We frequently observed such a thrust fault limited to one or two layers, associated with an incipient zone of folding. Only with geometric consideration, these folds are

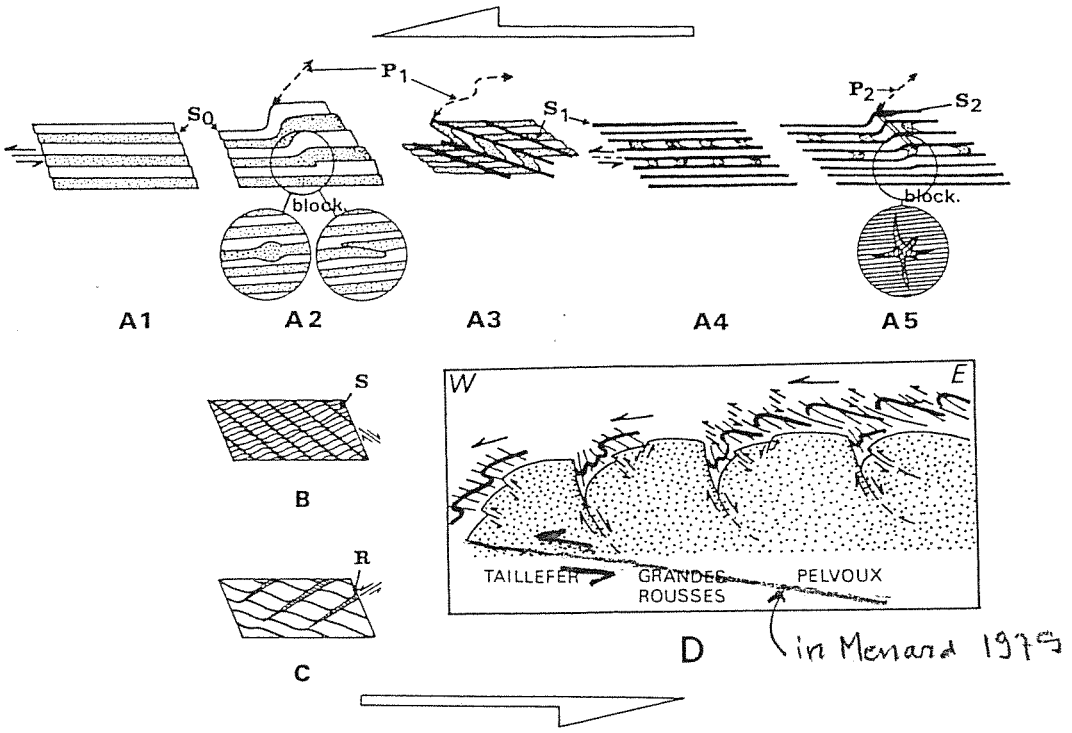

Fig. 14. Structures (fold of various symmetry and fracture) in a shear zone with change of thickness of the shear zone (see the text). A. S_0: strata; P_1S_1 first fold and cleavage; P_2S_2 second fold and cleavage, etc. Free slipping and shearing parallel to the main fabric in (A_1) and (A_4); local blocking or at least differential rate of displacement due to: heterogeneity, thrust fault in (A_2) or veins crossing S_1 in (A_5). B. S crenulation cleavage overprinting S_0, S_1, S_2, etc. C. R fracture overprinting S_0, S_1, S_2. D. Schematic E—W section of the Oisans massif. Dotted = basement; thick dashes = sedimentary cover; thin dashes = S_1 cleavage.

of drag type (Fig. 14A_2, and Fig. 4) when, at their initiation, the shear zone is thickened, or when the horizontal fold limb is thinner, due to adequate orientation of stress, favourable boundaries conditions and favourable rock behaviour. The stretching and slipping lineation is subperpendicular to the incipient fold axis. A slight elongation may exist parallel to this fold axis (Y direction). An increase of shear leads to amplification of these asymmetric folds (Fig. 14A_3 and center of the folded zone in Fig. 4) associated with a tilting of their axial planes which tend to become parallel to the previous fabric. The fold axes are reorientated and tend to become parallel to the stretching and slipping lineations (Fig. 14A_4) (Sanderson, 1973; Escher and Watterson, 1974; Carreras et al., 1977; Gratier et al., 1978; Bell, 1978; Quinquis et al., 1978).

The hinge of fold may migrate during this evolution (Robert, 1979). This

may explain the unrolling of striaes (and even of early X lineation) previously mentioned. At this moment (Fig. $14A_4$), the axial cleavage S_1 may have completely transposed the previous fabric (S_0). If the conditions for P_1 formation occur again (for example, by blocking on veins crossing S_1) a new asymmetric fold P_2 (drag fold type) appears (Fig. $14A_5$). A cycle is begun and may be repeated (S_2 transpose S_1, etc.). This succession of asymmetric folds can give a very important displacement only with internal strain in a shearing zone.

(2) The internal strain is expressed by asymmetric folds but with different asymmetries relatively to the previous case (Fig. 14B) when the shear zone is thinner or when the horizontal limb is thickened during deformation. By increasing of shear, the limbs are broken and the microlithons which appear from them, are tilted like playing cards in the opposite sense to the general shearing. Contrary to the previous case, this one implies a rapid blocking of the shearing. The movement must go on either by a migration of the affected zone, or on new discontinuities as a third case:

(3) If rupture occurs in the shearing zone (behaviour change of rocks for example by fluid migration, at the end of the deformation: Vialon, 1974a, or by transfer process); they may be arranged like Riedel fractures. If the general decrease in thickness of the shear zone is small, the movement on these fractures is small too; these fractures open out and are filled with minerals. If the thickness strongly decreases, the blocks slip on one another with elongation parallel to the X-direction.

Most of the structures (with inclined S_1) described in the cover of the external basement of the Alps, may be explained by the succession of some of these three cases. Generally, the first case (Fig. $14A_3$) occurred, with asymmetric folds P_1 (and S_1 cleavage). Then, according to the regional situation and to the nature of rocks, we have either asymmetric folds P_2 of the first case (Fig. $14A_3$) or asymmetric folds P_2 of the second case (Fig. 14B) — both with S_2 cleavage. The S_2 cleavage of the second case (Fig. 14B) is associated with conjugate fractures of Riedel type (Fig. 14C), this system being asymmetrical with respect to the shear plane.

Regional interpretations

The previous partial interpretation has allowed us to define particular mechanisms relative to two different dips of the S_1 cleavage (vertical and inclined). But the dip of S_1 continuously varies from east to west and this must be integrated in a global regional mechanism.

The vertical pinched synclines between wider anticlines of the basement-cover boundary, immediately suggest a horizontal E—W contraction on the E—W section of the Oisans massif (Fig. 1). But observations in a tunnel through the Belledonne massif show that the axial plane of the pinched synclines tend to become horizontal with depth. On the other hand, near the actual erosion surface, this syncline exhibits an asymmetrical structure with

differences from east to west for each syncline (Fig. 1):

On the eastern part, the structures may be matched with model A of Fig. 14. The assymetric P_1 folds pass into nappes when their axial planes become thrust planes with lamination of the overturned limb (Fig. 14D). Uplift and thrusting of the basement (over the cover or within the basement massif: Pecher, "Geological map of St Christophe en Oisans", 1978) are associated with these folds. This implies a shearing deformation parallel to the basement cover boundary with the upper part moving to the west (as previously mentioned, along the décollement surface between cover and basement).

On the central and western part, S_1 is vertical. There is an uplift of the western basement, along a great fault, with lamination of the cover and with alpine cleavage in the basement near this fault (Fig. 14D). This fault may be interpreted as a cleavage plane like those of model B (Fig. 14). It may be associated with a shearing displacement as for the eastern part of each syncline.

Thus all the structures in the sedimentary cover of Oisans may be attributed to a progressive deformation with subhorizontal east—west contraction and shearing parallel to the basement cover boundary, the upper part moving westward.

This simplified model is more complex in detail: The initially subhorizontal surface of the basement cover boundary may vary due to transverse folds (Cretaceous) prior to the P_1S_1 folding (Gratier et al., 1973). The EW contraction also varies according to the shape of the basement blocks, which are moving each against the other. These blocks are bounded by wrench fault which contribute towards the general curvature of the Alpine arc, of which the Pelvoux massif is the core (Vialon, 1974b; Boudon et al., 1976; Robert and Vialon, 1976; Tricart et al., 1977; Menard, 1979).

CONCLUSIONS

The folding of the basement-cover boundary (pinched synclines and wide anticlines) is attributable to a progressive deformation with subhorizontal E—W contraction and shearing parallel to the basement cover interface (upper part moving to west). During this deformation, the temperatures varied from 350° (near the basement) to 250°, and the fluid pressure from 200 to 250 MPa. The observed characteristic examples of the behaviour of an heterogeneous material during coaxial and non-coaxial deformation are:

(1) The basement is deformed (cleavage) in tight strips near the pinched cover syncline. In the eastern part of each syncline, the basement thrusts and is associated with asymmetrical folds and nappes in the cover.

(2) Indentation exists on all scales: hard objects in initial homogeneous matrix (with parenthesis form of pressure solution cleavage); basement block limited by wrench and thrust faults (with variation of strain value in the cover).

(3) The deformation is inhomogeneous. The estimation of a volume

change using the strain value is not a simple matter. The most strained zones often become discontinuity planes with slip.

(4) The orientation of each structure is strongly affected by the attitude of the boundary of an adjacent heterogeneity.

(5) The cover is folded and cleaved, and its characteristics (attitudes, amplitudes, symmetry, etc.) vary from place to place. In all cases, initially the folds axes were horizontal and parallel to a slight elongation (Y). Throughout the deformation, the X direction remained vertical (upright fold) or in a vertical E—W plane (inclined folds). The fold axes tended to become parallel to the X direction with increase of the X/Z and X/Y ratio (with reorientation of all previous structures).

(6) In a non-coaxial progressive deformation appears: successive superposition of different asymmetric folds, successive cleavage (transposition), successive fractures (Riedel). This is related to a progressive shear-deformation when the initial shear plane is parallel to the main planar anisotropy (S_0 at first, S_1 after, then S_2, etc.) with variation of thickness of the shear zone but constant "a" direction of shearing.

(7) In such a non-coaxial deformation, the evolution of the cleavage is dependent on the relations between the rate of rotation of contraction direction (Z) and the rate of the cleavage process: (a) the cleavage remains always perpendicular to the Z direction; (b) shearing and/or slipping occurs parallel to the initial cleavage plane; (3) the initial cleavage is obliquely overprinted by a new crenulation cleavage.

ACKNOWLEDGMENTS

The critical comments, and language corrections, by P.R. Cobbold have greatly helped the authors in improving this paper. The authors thank also A. Pecher and colleagues of the I.R.I.G.M. where this work was carried out. This paper is an I.R.I.G.M. contribution. 78-TECT. Nr. 5.78. Financial support of this study was provided by ATP INAG Nr. 35-30.

REFERENCES

Allirot, D., Boehler, J.P., 1976. Déformation plastique expérimentale des roches anisotropes. Bull. Soc. Géol. Fr., 7, XVIII (6): 1539.

Autran, A., Fonteille, J., Goguel, J. and Guitard, G., 1975. Sur le mécanisme de la schistosité. Jubilee Vol., Soc. Géol. Belg, pp. 89—121.

Ayrton, S.N., 1972. La Croix de Fèr, Trient. La signification d'une structure verticale. Bull. Soc. Vaud. Sci. Nat., 71 (6): 345—346.

Ayrton, S.N. and Ramsay, J.G., 1974. Tectonic and metamorphic events in the Alps. Schweiz. Mineral. Petrogr. Mitt., 54 (2/3): 609—639.

Badoux, H., 1963. Les Bélemnites tronçonnées de Leytron (Valais). Bull. Lab. Géol. Min. Géophys. Mus. Géol. Univ. Lausanne, 138: 1—3.

Bell, T.H., 1978. Progressive deformation and reorientation of fold axes in a ductile mylonite zone: the Woodroffe thrust. Tectonophysics, 44 (1—4): 285—320.

Bernard, D., 1978. Microthermométrie des Inclusions fluides de Cristaux syncinéma-

tiques. Application à la Couverture sédimentaire du Nord Pelvoux. Thesis, University of Grenoble, Grenoble.
Bernard, D., Gratier, J.P. and Pecher, A., 1977. Application de la microthermométrie des inclusions fluides des cristaux syncinématiques à un problème tectonique. C.R. Somm. Séances Soc. Géol. Fr., 5: 284—288.
Boudon, J., 1976. Application de la Méthode des Éléments finis à l'Approche mécanique d'un Phénomène tectonique, le Poinçonnement (cas d'une Couverture sédimentaire déformée par un Mouvement d'un Compartiment de Socle). Thesis, University of Grenoble, Grenoble.
Boudon, J., Gamond, J.F., Gratier, J.P., Robert, J.P., Depardon, J.P., Gay, M., Ruhland, M. and Vialon, P., 1976. L'arc alpin occidental: réorientation de structures primitivement EW par glissement et étirement dans un système de compression NS? Eclogae Géol. Helv., 69 (2): 509—519.
Brun, J.P., 1978. Le problème de l'interprétation des directions "a" déterminé par l'étude des linéations déformées. Géol. Rundsch., 67 (1): 305—313.
Carreras, J., Estrada, A. and White, S., 1977. The effects of folding on the C-axis fabric of a quartz mylonite. Tectonophysics, 39 (1—3): 3—24.
Choukroune, P. and Lagarde, J.L., 1977. Plan de schistosité et déformation rotationnelle: exemple du gneiss de Champtoceaux Massif Armoricain. C.R. Acad. Sci., 284 D: 2331—2334.
Cobbold, P.R., 1976. Fold shapes as function of progressive strain. Philos. Trans R. Soc., London, Ser. A., 283: 129—138.
Escher, A. and Watterson, J., 1974. Stretching fabrics, folds and crustal shortening. Tectonophysics, 22: 223—231.
Gratier, J.P., 1976. Déformation et changement de volume dans un marbre à stylolithes de la région de Rabat (Maroc). Bull. Soc. Géol. Fr., 7, XVIII (6): 1461—1469.
Gratier, J.P., 1979. Mise en évidence de relations entre changement de composition chimique des roches et intensité de leur déformation. Bull. Soc. Géol. Fr., XXI (1): 95—104.
Gratier, J.P. and Vialon, P., 1975. Clivage schisteux et déformations: analyse d'un secteur clé du bassin mésozoïque de Bourg d'Oisans (Alpes Dauphinoises). Géol. Alp., 51: 41—50.
Gratier, J.P., Lejeune, B. and Vergne, J.L., 1973. Etude des déformations de la Couverture et des Bordures sédimentaires des Massifs cristallins externes de Belledonne, des Grandes Rousses et du Pelvoux. Thesis, University of Grenoble, Grenoble.
Gratier, J.P., Boudon, J., Gamond, J.F., Plotto, P., Robert, J.P., Vialon, P., 1976. Les variations longitudinales des valeurs d'aplatissements du synclinorium de Bourg d'Oisans (Alpes Dauphinoises) — Méthode de mesures et résultats. Réun. Annu. Sci. Terre, 4e, Paris.
Gratier, J.P., Pecher, A. and Vialon, P., 1978. Relation entre déformation interne et déplacement — Glissement dans les roches anisotropes. Mém. B.R.G.M., 91: 207—214.
Hansen, E., 1971. Strain Facies. Allen and Urwin, London, 207 pp.
Hobbs, B., Means, W. and William, P., 1976. An Outline of Structural Geology. Wiley, New York, N.Y., 571 pp.
Le Corre, Cl., 1978. Approche quantitative des Processus synschisteux. Thesis, University of Rennes, Rennes.
Masson, H., 1971. Sur les mesures de la déformation dans les roches à linéation (échantillonnage de polarité mixte). Bull. Soc. Vaudoise Sci. Nat., 71 (337): 1—23.
Ménard, G., 1979. Relations entre Structures profondes et Structures superficieles dans le SE de la France. Essai d'Utilisation de Données géophysiques. Thesis, University of Grenoble, Grenoble.
Pecher, A., 1978. Carte géologique de St Christophe en Oisans 1/50.000.
Pijolat, B., 1978. Les déformations des Terrains secondaires de la Région de Megève

(Haute Savoie). Mise en Evidence d'une Zone de cisaillement dans un Plan horizontal. Thesis, University of Lyon, Lyon.
Plotto, P., 1977. Structures et Déformation des Grès du Champsaur au SE du Massif du Pelvoux. Thesis, University of Grenoble, Grenoble.
Poty, B., Stalder, H.A. and Weisbrod, A.M., 1974. Fluid inclusion studies in quartz from fissure of Western and Central Alps. Schweiz. Mineral. Petrogr. Mitt., 54 (2/3): 717—752.
Quinquis, H., Audren, C., Brun, J.P. and Cobbold, P.R., 1978. Intense progressive shear in Ile de Groix blue schists and compatibility with subduction or obduction. Nature, 273: 43—45.
Ramsay, J.G., 1967. Folding and Fracturing of Rocks. Mac-Graw Hill, New York, N.Y., 565 pp.
Rhodes, S. and Gayer, R.A., 1977. Non-cylindrical fold, linear structures in the X direction and mylonites developed during translation of the Caledonian Kalak Nappe Complex of Finnmark. Geol. Mag., 114 (5): 329—408.
Robert, I., 1979. Etude de Mécanismes de Plissements d'une Serie regulièrement stratifiée (Exemple de la Côte Basque). Thesis, University of Grenoble, Grenoble.
Robert, J.P. and Vialon, P., 1976. Déformation interne et déformation aux limites dans un assemblage de blocks découpés par un cisaillement. Le clivage schisteux des niveaux structuraux supérieurs. Bull. Soc. Géol. Fr., 7, XVIII (7): 1599—1604.
Sanderson, D.J., 1973. The development of fold axes oblique to the régional trend. Tectonophysics, 15 (1/2): 55—71.
Smith, J.V. and Strenstrom, J.C., 1965. Electron excited luminescence as a petrologic tool. J. Geol., 73: 627—635.
Tricart, P., Caron, J.M., Gay, M. and Vialon, P., 1977. Relais des schistosité, structures en éventail et discontinuités majeures sur la transversale du Pelvoux. (Alpes Occidentales). Bull. Soc. Géol. Fr., XIX (4): 873—881.
Vialon, P., 1968. Clivage schisteux: répartition et genèse dans le bassin mésozoïque de Bourg d'Oisans. Trav. Lab. Géol. Grenoble, 44: 353—366.
Vialon, P., 1974a. L'importance du changement de comportement mécanique du matérial au cours d'une déformation unique, dans la définition des superpositions de structures et de phases tectoniques. Exemple de clivage schisteux. Réun. Sci. Terre, 2e, Nancy.
Vialon, P., 1974b. Les déformations synschisteuses superposées en Dauphiné, leur place dans la collision des éléments du socle préalpin. Conséquences pétrostructurales. Schweiz. Mineral. Petrogr. Min., 54 (2/3): 663—690.
Vialon, P., Ruhland, M. and Grolier, J., 1976. Eléments de tectonique analytique. Masson, Paris, 118 pp.